Journal of Power Sources 213 (2012) 223–228

Contents lists available at SciVerse ScienceDirect

Journal of Power Sources

journal homepage: www.elsevier.com/locate/jpowsour

Nd-nickelate solid oxide fuel cell cathode sensitivity to Cr and Si contamination

J. Andreas Schuler [a,b,*], Henning Lübbe [a,c], Aïcha Hessler-Wyser [b], Jan Van herle [a]

[a] Laboratoire d'Energétique Industrielle (LENI), Ecole Polytechnique Fédérale de Lausanne (EPFL), CH-1015 Lausanne, Switzerland
[b] Centre Interdisciplinaire de Microscopie Electronique (CIME), Ecole Polytechnique Fédérale de Lausanne (EPFL), CH-1015 Lausanne, Switzerland
[c] Laboratoire de Technologie des Poudres (LTP), Ecole Polytechnique Fédérale de Lausanne (EPFL), CH-1015 Lausanne, Switzerland

ARTICLE INFO

Article history:
Received 6 December 2011
Received in revised form
28 March 2012
Accepted 30 March 2012
Available online 25 April 2012

Keywords:
Solid oxide fuel cell (SOFC)
Cathode
Nickelate
Cr-poisoning
Contamination
Silicon

ABSTRACT

The stability of Nd-nickelate, considered as an alternative solid oxide fuel cell (SOFC) cathode material, was evaluated in this work on its tolerance towards contaminants.

Symmetrical cells with $Nd_{1.95}NiO_{4+\delta}$ (NNO) electrodes sintered on gadolinia-doped ceria electrolyte supports were monitored over time-spans of 1000 h at 700 °C under polarization in an air-flux with deliberate chromium contamination. Impedance spectroscopy pointed out a polarization increase with time by the growth of the low frequency arc describing the electrode's oxygen reduction and incorporation processes.

Post-test observations revealed polluted cathode regions with increasing amounts of Cr accumulations towards the electrolyte/cathode interface. Cr deposits were evidenced to surround active nickelate grain surfaces forming Nd-containing Cr oxides.

In addition to exogenous Cr contamination, endogenous contamination was revealed. Silicon, present as impurity material in the raw NNO powder (introduced by milling during powder processing), reacts during sintering steps to form Nd-silicate phases, which decreases the active cathode surface.

Nd-depletion of the nickelate, as a result of secondary phase formation with the contaminants Cr and Si ($NdCrO_4$ and $Nd_4Si_3O_{12}$), then triggers the thermally-induced decomposition of NNO into stoichiometric $Nd_2NiO_{4+\delta}$ and NiO.

Summarized, the alternative Nd-nickelate cathode also suffers from degradation caused by pollutant species, like standard perovskites.

1. Introduction

The oxygen-overstoichiometric Nd-nickelate $Nd_2NiO_{4+\delta}$ structure is described as alternatingly stacked perovskite- and rock-salt-like layers, as the first member of the Ruddlesden–Popper series $A_{n+1}B_nO_{3n+1}$. Contrarily to perovskite-based cathode materials, which generally need A-site doping (usually by Sr) to generate oxygen nonstoichiometry under certain conditions of temperature and oxygen partial pressure, oxygen can incorporate into the nickelate structure giving mixed electronic and ionic conductivity already at low temperature in air. Nd-nickelate is thus seen as an intermediate-temperature solid oxide fuel cell (IT-SOFC) electrode material alternative to perovskites [1].

Under SOFC operating conditions, volatile chromium species emanate from cell-proximal Cr-containing materials and accumulate at the active cathode sites for oxygen reduction, leading to polarization losses and performance decrease. An alternative composition free of strontium and manganese, is suggested to mitigate the extent of this degradation [2] – so-called Cr-poisoning [3]. Nickelate cathodes are supposedly more tolerant to Cr-poisoning, as indicated by a recent study [4], where only a negligible chemical oxygen surface exchange coefficient decrease was measured for Nd-nickelate material after exposure to Cr (10 nm thick Cr-layer on NNO). Investigations of Cr-poisoning in such cathodes are, however, scarce; the present work aims to contribute to this topic by testing $Nd_{1.95}NiO_{4+d}$ electrodes under deliberate Cr contamination conditions.

Cr-poisoning conditions are created here by humidifying the air fed to the cathode, preheated in a Cr-containing alloy tube, as the partial pressure of Cr-oxyhydroxide $CrO_2(OH)_2$ species is proportional to the water vapour pressure [1,5]. To isolate the effects due to Cr, the tested cathode material should be tolerant to water

* Corresponding author. Laboratoire d'Energétique Industrielle (LENI), Ecole Polytechnique Fédérale de Lausanne (EPFL), CH-1015 Lausanne, Switzerland. Tel.: +41 21 693 4827; fax: +41 21 693 3502.
E-mail address: andreas.schuler@epfl.ch (J. Andreas Schuler).

0378-7753/$ – see front matter © 2012 Elsevier B.V. All rights reserved.
doi:10.1016/j.jpowsour.2012.03.112

vapour at operating temperature to avoid superimposed effects of humidity on the cathode performance. Recently, Nd-nickelates were reported to show high stability in H_2O-containing atmospheres [6,7] even if a decrease of 1 order of magnitude (low compared to standard perovskites) of the chemical surface exchange coefficient of oxygen was found after long-term (1000 h) testing [8]. Therefore, the use of Nd-nickelate cathodes in Cr-poisoning conditions with humid air is assumed to be possible here for reasonable time-spans.

2. Scientific approach

In the ongoing parallel work, the authors aim to develop a cathode supported microtubular SOFC using porous Nd-nickelate as the support tube, co-fired with thin dense gadolinia-doped ceria/scandia-stabilized zirconia double electrolyte layers [9]. To achieve densification of the electrolytes, the present target sintering temperature is 1573 K. In this work, examining at the outset the Cr-tolerance of the nickelate material, simpler samples were fabricated, that mimic the cathode side of the future microtubular fuel cells: symmetrical Nd-nickelate layers were deposited on sintered thick ceria-gadolinia pellets at the same firing temperature (1573 K), with one side subsequently exposed to Cr-containing air under polarization for ca. 1000 h, and finally post-analyzed. The analysis revealed several side reactions, originating from the starting powder and the high temperature step, which explain poor electrode performance. The emphasis in this article is therefore not the nickelate performance as cathode, but the results obtained from post analysis, which indicate the improvement steps required for further development of this system. The electrochemical testing should therefore be seen as a means to obtain cathode overpotential-driven C-poisoning, i.e. Cr deposition in the electrochemically active cathode, and not focusing on absolute performance.

3. Experiments

The studied samples are symmetrical cells of Nd-nickelate electrodes on thick (1 mm, 94% dense) electrolyte supports. The latter were fabricated by uniaxial compression of $Ce_{0.9}Gd_{0.1}O_{1.95}$ (GDC, *Nextech*, USA) powder within a 24 mm diameter mould by applying a pressure of 44 MPa prior to a sintering step of 120 min at 1573 K in air. Circular $Nd_{1.95}NiO_{4+\delta}$ (NNO, *Marion Technologies*, France) electrodes of 8 mm diameter were screen-printed on both sides of the GDC support, according to an experimental protocol described elsewhere [10], followed by a sintering step of 60 min at 1573 K, leading to an electrode thickness of ca. 15 μm. Subsequently, a gold grid was sintered on the NNO cathode at 1313 K while applying a load of ca. 250 g. The NNO powder presented an unwanted silicon (Si) impurity content up to 1.5 at% in the as-received state, introduced before the final milling and detected only later on. An NNO-based reference electrode was likewise deposited onto the support; the positioning on the solid electrolyte followed proposals by Nagata et al. [11] for accurate electrochemical impedance spectroscopy measurements (EIS). The gold grids were connected to a galvanostatic device using gold wires; the counter and reference electrodes were additionally covered with an unsintered $La_{0.7}Sr_{0.3}CoO_3$ (LSC, *Praxair*, USA) contacting layer for better current collection; this was avoided for the Cr-exposed NNO working electrode so as not to influence its reaction by the presence of another material. The absence of such a better current collection layer, which in addition may participate in the electrochemical reaction, contributed to higher losses overall, which was confirmed from parallel tests including LSC current collection, not reported here.

The symmetrical cells were kept in a furnace at 973 K, polarized for 1000 h with a constant current load of 0.5 A cm^{-2}, while monitoring the potential between the electrodes. Polarization was occasionally switched off for EIS measurements, performed on an *IM6* impedance analyzer (*Zahner*, DE) with *Thales 2.15* software. The cathode was fed with a 0.4 L min^{-1} air-flux, heated within a tubing element made of Inconel 600 (NiCrFe) alloy for deliberate emission of volatile Cr species. This experimental arrangement does not allow for comparison with a baseline test without Cr contamination; despite this drawback, the setup allows homogeneously distributed delivery of gaseous Cr species to the button cell cathode and therefore to study this particular effect, especially from post-test analysis. Fig. 1 provides a schematic illustration of the test setup. The water vapour pressure was 1.8×10^2 Pa when using dry (compressed) air, and 3.0×10^3 Pa in humidified conditions (bubbled through a water bottle). The partial pressures of volatile Cr are estimated from comparison with a similar experiment using Inconel 602 alloy [12], where they are close to saturation pressures, which are 5.5×10^{-5} and 9.2×10^{-4} Pa, in dry and humidified air respectively.

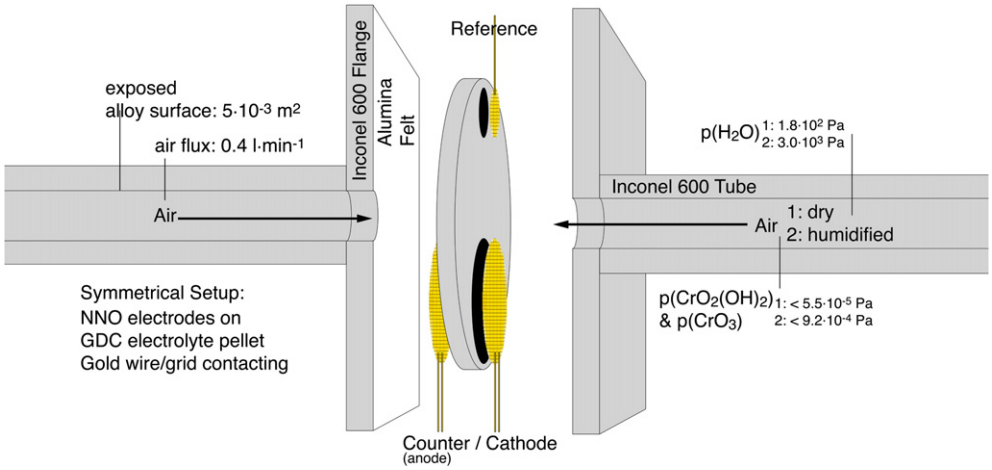

Fig. 1. Schematic illustration of the testing arrangement, where symmetrical cells are placed between two metallic flanges covered with alumina felts. The flange-ending pipes ensure air feed, heat exchange, contacting (compression by calibrated springs) and deliberate Cr-poisoning conditions. Switching the air feed from dry to humidified air changes the Cr contamination levels as indicated on the figure.

Analyses of post-test and fresh samples included X-ray diffraction (XRD), which were performed on a *D8* diffractometer (*Bruker*, DE), and energy-dispersive X-ray spectroscopy (EDS) on both scanning and transmission electron microscopes (SEM/STEM). Post-test analyses and sample preparation protocols, like embedding, cross-section cutting, polishing and focused ion beam (FIB) TEM-lamellae preparation steps are described elsewhere [13].

4. Results and discussion

Two symmetrical cells were successively monitored under current load at operating temperature. Apparently stable performance, even slightly improving, was observed by voltammetry, during testing in dry air (see Fig. 2, first cell) as well as in both dry and humidified air (see Fig. 3, second cell) over time-spans of 1000 h. An ohmic resistance of ca. 3.6 Ω can be attributed to the electrolyte, supposing 0.055 S cm^{-1} for the conductivity of GDC at 973 K [14] and taking into account the electrolyte's porosity [15]. As mentioned before, the absolute performance being poor, we focus here on the relative performance evolution with respect to the presence of Cr contamination, in combination with post-test analysis.

4.1. Electrochemical behaviour

To focus on the relative electrode response with time, EIS measurements are reported under zero current bias in Figs. 2and 3 for both cells. EIS recording under bias was noisy and the variations small; one notices in fact that overall DC performance at 0.5 A cm is rather stable (Figs. 2a and 3a). Initial spectra for NNO cathodes (see Fig. 2C), taken before ageing, reveal two major contributions: a medium frequency arc around 10^4 Hz and a low frequency arc around ca. 10^2 Hz, representing processes at the cathode/electrolyte interface and oxygen reduction at the cathode/air interface, respectively, according to Mauvy et al. [16].

Equivalent circuit fitting on EIS spectra evidenced an increase of the low frequency contribution with polarization time, likely indicating the effect of Cr-contaminating conditions besides other possible electrode altering phenomena on the catalytic properties of NNO for oxygen reduction discussed further below. The relatively stable performance at 0.5 A cm bias indicated by voltammetry (see Figs. 2A and 3A) could be explained by the intrinsic mixed conductivity of NNO delocalisable throughout the cathode thickness. Cr deposits observed close to the interface (shown further below) likely constrict total current but do not block it. Furthermore, the ohmic contribution decreases with time, visible from the high frequency intercept, in part balancing the polarization resistance increase. This ohmic decrease is probably due to contact improvement, i.e. sintering of the gold mesh and increasing contact points.

Spectra at 500 h and 530 h in Fig. 3B indicate no significant change in impedance behaviour under higher water vapour pressure, which would confirm the supposed relative tolerance of NNO cathode material towards H_2O [6,7]. Also, no change in slope during polarization is observed when switching from dry to humidified gas (see Fig. 3a). Thus, although higher amounts of Cr are fed to the cathode with humidified gas, the rate of Cr accumulation at active cathode sites appears to be constant, underlining a Cr deposition process driven by the electrochemical reduction of volatile $Cr^{(VI)}$ species [3].

4.2. Cr contamination

For the interpretation of cathode behaviour under deliberate Cr-contaminating conditions, and likely affecting the cathode performance with time, post-test analyses were conducted on cathodes. Distributions of Cr accumulations through the cathode thickness were obtained by extracting Cr concentrations from EDS spectra of 1 μm thick cathode slices, similarly to the Cr quantification methodology described elsewhere [12,17]. Fig. 4 shows the Cr-profile

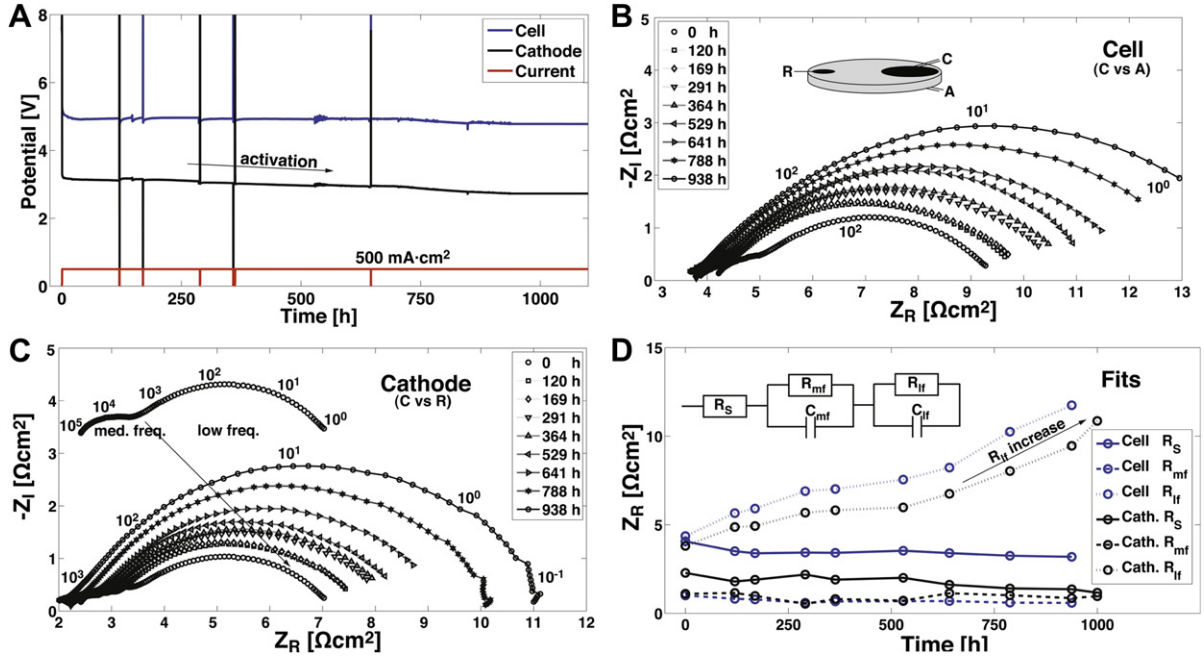

Fig. 2. [A] Cell and cathode potential (vs reference) evolution with time in DC conditions at 0.5 A/cm show an apparent degradation-free behaviour. Impedance spectra (at zero bias current) evidence an increase of polarization resistance with time. For both the symmetrical cell [B] and the cathode [C] the evolution of resistive contributions, obtained by fitting a simple equivalent circuit on EIS spectra [D], underline an increase of the low frequency arc (R_{lf}), which describes oxygen reduction on the electrodes, whereas small decreases of the ohmic and the medium frequency cathode/electrolyte interface contributions are observed.

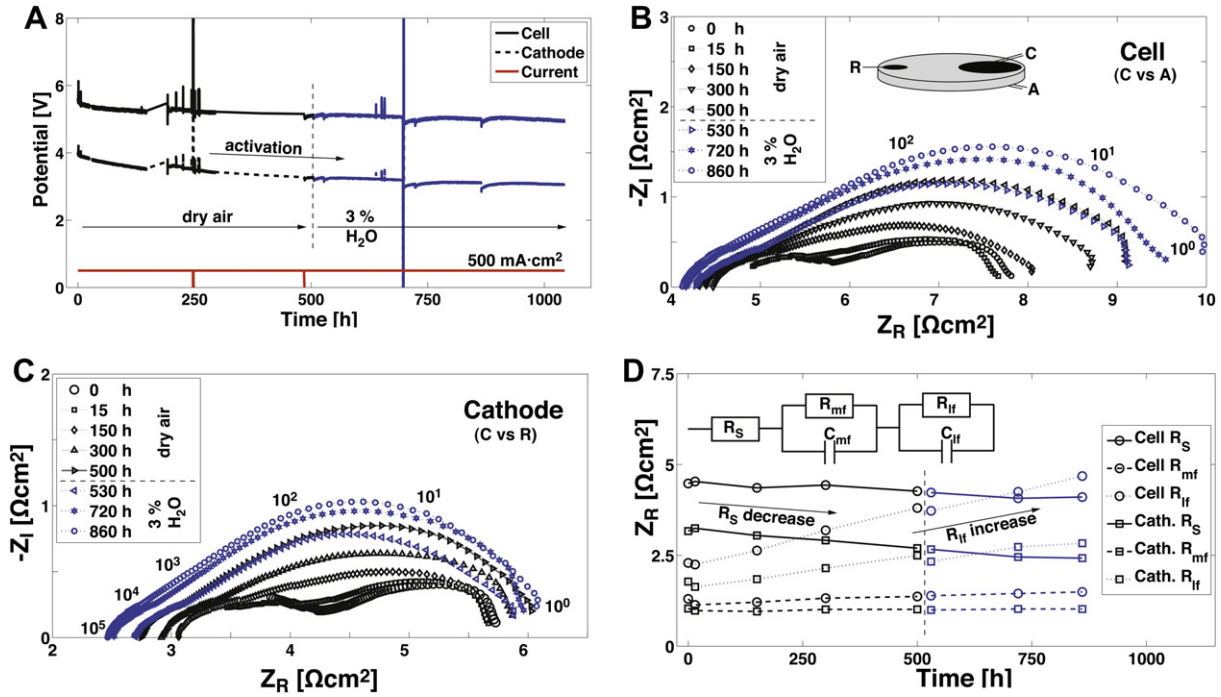

Fig. 3. [A] Evolution of cell (C vs A) and cathode (C vs R) potentials under polarization at a current load of 500 mA cm^{-2} under dry and humidified air. [B] Impedance spectra of the symmetrical cell and [C] the cathode; the last three acquisitions were performed under higher water vapour conditions to the cathode (second part, ≥500 h, of the test). The cathode contribution to resistivity is marked by an increase of polarization resistance partly counterbalanced by contact improvement. [D] EIS fitting with a simple equivalent circuit-based model underlines this observation.

superimposed to the SEM-FIB image on the left. The Cr distribution shows a rather slowly decaying profile over 7 μm, as opposed to a much steeper profile observed for (La,Sr)MnO_3/Y–ZrO_2 cathodes, with Cr accumulating towards the electrolyte interface [12]. This observation corroborates the spreading of the reaction zone into the nickelate cathode thickness, as expected for materials with mixed ionic and electronic conductivity.

To identify the nature of Cr accumulations more closely, a TEM-lamella (cf. Fig. 4, right) was prepared by FIB extraction from the electrolyte/cathode interface. At higher magnification, STEM-EDS results, given on the right of Fig. 4 together with the elemental maps, revealed Cr in combination with Nd, in the form of Nd-chromate, $NdCrO_4$. The latter is the thermodynamically favored phase of the Nd–Cr–O system under cathode operating conditions

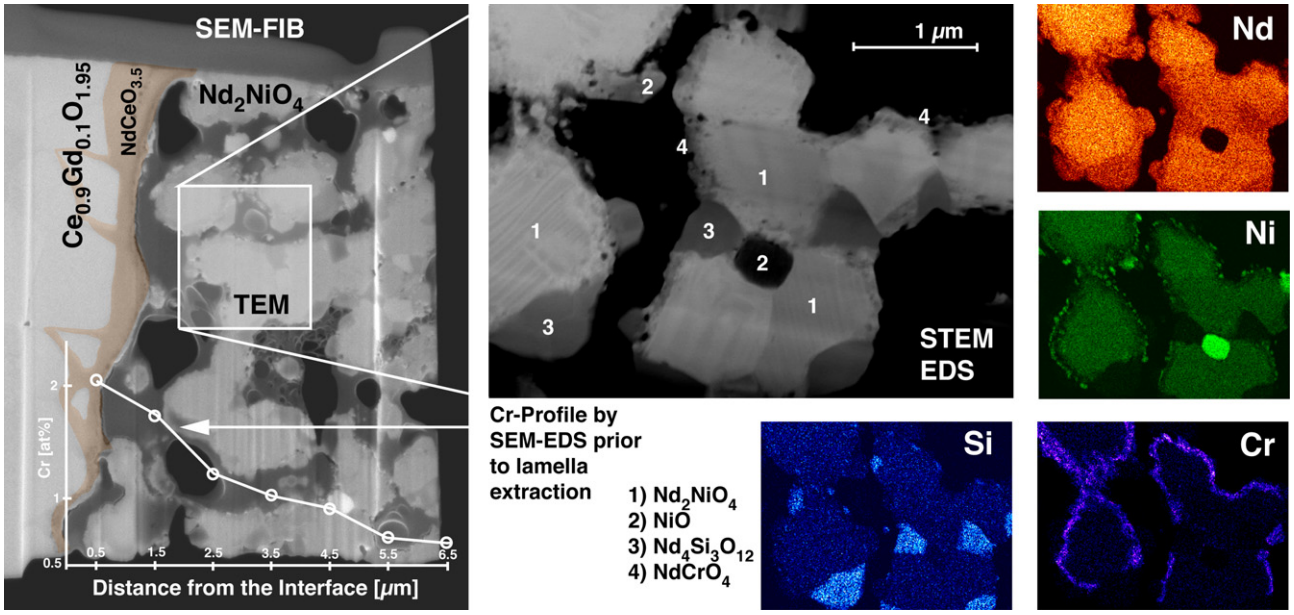

Fig. 4. Left: the SEM imaging of a TEM-lamella, extracted by FIB from the cell described in Fig. 2, shows an NNO cathode region on a GDC support with an intermediate $NdCeO_{3,5}$ reaction layer. A Cr profile through the cathode thickness is superimposed to the bottom of the SEM-FIB picture; the profile was obtained by extracting Cr concentrations from 1 μm cathode slices from EDS spectra. Right: the dark STEM image and corresponding EDS elemental maps, from the central part of the FIB-lamella from the left side of the picture, reveal Cr deposits on active NNO grain surfaces as well as secondary Ni- and Si-rich phases.

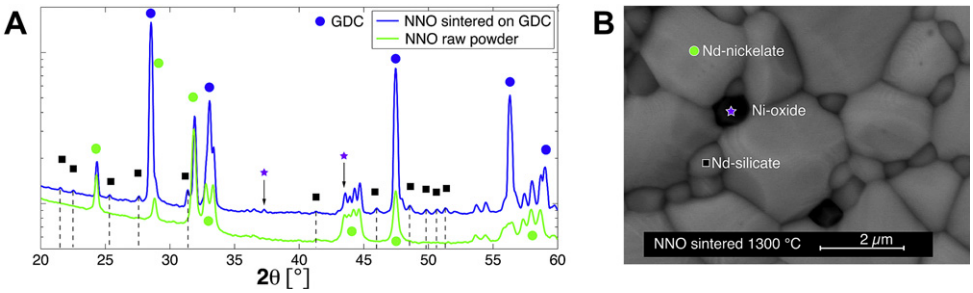

Fig. 5. [A] The changes in XRD spectra between raw and sintered NNO (Nd_2NiO_4 00-021-1274, green circle symbol) powder indicates Nd-silicate $Nd_4Si_3O_{12}$ (00-042-0171, black square symbol) to originate from amorphous Si impurity. NiO (00-078-0429, purple star symbol) phase appears also after the high temperature step. The pattern corresponding to GDC($Ce_{0.8}Gd_{0.2}O_2$ 00-050-0201, blue circle symbol) stems from the electrolyte support. The numbers in brackets are ICDD references. [B] The BSE-SEM image of sintered NNO powder clearly reveals the thermally-induced NNO (large grains) decomposition into NiO (small black grains) triggered by the Si contamination-caused Nd-silicate (small grey grains) formation. (For interpretation of the references to colour in this figure legend, the reader to the web version of this article.)

[18]. The Cr-rich phases decorate the active NNO particle surfaces, indicating again the mixed conductivity of NNO.

This result is in clear opposition with a supposed Cr-tolerance of NNO, free of Sr and Mn. Considering that a decrease (40%) in chemical oxygen surface exchange coefficient was reported for 20 nm Cr deposits on the NNO surface and 2000 h testing time [4], the ca. 100 nm thick Cr phases observed here are therefore believed to be at least in part responsible for the cathode performance decrease seen in the EIS measurements.

4.3. Additional contamination

Besides Cr, silicon contamination was revealed to a significant extent in post-test samples. Although XRD measurements on raw powder had not revealed patterns corresponding to Si-phases (cf. Fig. 5[A]), Si was identified by EDS in the delivered powder. Silicon therefore seems to be present as amorphous material and had been introduced by milling during powder processing for particle size reduction. The XRD measurements (Fig. 5[A]), as well as STEM-EDS (Fig. 4 right) and SEM-BSE (Fig. 5[B]) images taken on sintered and post-test cathodes allowed to identify Nd-silicate as thermally-induced reaction phase. The deleterious effect of Si-poisoning is obvious, as the $Nd_4Si_3O_{12}$ phase decreases the number of active cathode sites. The absence of Cr around the silicate phase surfaces, clearly visible from Cr and Si EDS maps in Fig. 4 strengthens these findings; if the $Nd_4Si_3O_{12}$ phase were active for oxygen reduction, the Cr deposits would have been expected here as well.

Finally, sulfur-rich phases were identified by SEM-EDS (not presented here) as reaction products of NNO cathode material with SO_2 present to 10 ppb in urban air [5], which accumulate in long-term tests. Nickelate seems therefore not tolerant to sulfur contamination either, similar to reactive perovskites, that form sulfates [19].

4.4. Synergistic degradation effects

NiO precipitates illustrated in Fig. 4[right] and Fig. 5B suggest a contamination-induced decomposition of the nickelate structure. As Nd-deficient nickelate tends to transform into Nd_2NiO_{4+d} and NiO, the initial Si contamination of the raw powder leads to additional Nd-deficiency (by Nd-silicate formation) and so to enhanced NiO precipitation during high temperature cathode sintering. A

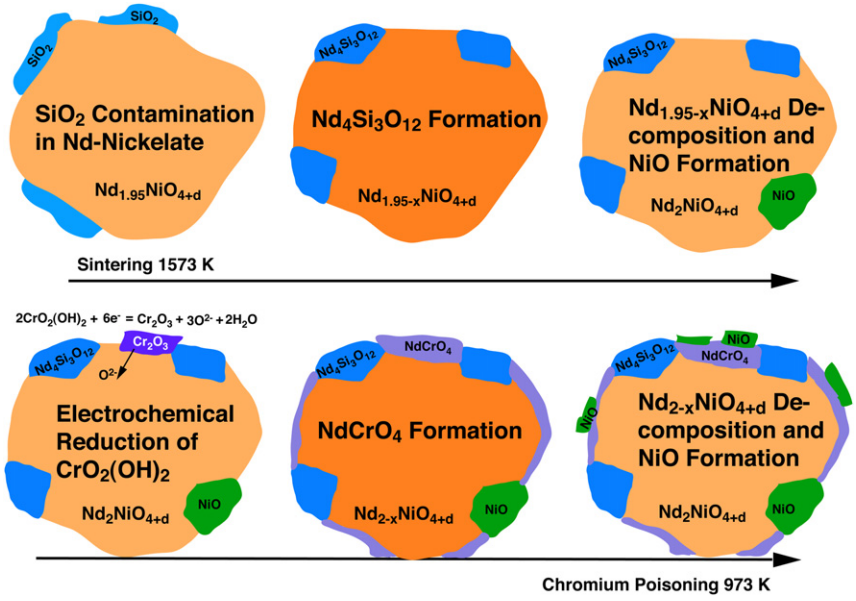

Fig. 6. Decomposition of Nd-deficient nickelate into the more stable stoichiometric phase and Ni oxide are triggered by a Si contamination-induced Nd-depletion during the high temperature sintering step; Cr-poisoning during electrochemical polarization, i.e. Cr deposition on active NNO surfaces and involving Nd-chromate formation, leads to further Nd-depletion and decomposition of the NNO phase.

degradation mechanism of Si-contaminated NNO powder, suggested from the findings in this work, in addition to observations from a previous study in ref. [20], is illustrated in Fig. 6. Bulky NiO grains are suggested to have their origin in electrode preparation and not in high overpotential at the cathode under polarization.

During Cr-poisoning, the reductive deposition of volatile Cr species in form of Cr_2O_3 and its subsequent reaction with nickelate to form $NdCrO_4$ compounds induces additional Nd-depletion of NNO and leads to precipitation of NiO as suggested in Fig. 6 and evidenced in the Ni mapping of Fig. 4[right].

Fig. 4[left] moreover shows a reaction layer between NNO and GDC materials. The GDC electrolyte is meant to act as a reaction buffer layer between NNO and zirconia-based electrolyte materials, which would react severely, to produce full microtubular cells based on porous nickelate support tubes. In order to simulate the co-sintering process of nickelate tubes and the electrolyte layers, the electrodes were sintered at 1300 °C, believed to be the limiting fabrication temperature for the tubular SOFC. This study shows a marked interfacial Nd-cerate $NdCeO_{3,5}$ reaction phase [21]; additional reactivity studies showed this phase to appear during high temperature treatments (sintering) of the combination of NNO and CGO materials and not to evolve under IT-SOFC operating temperatures. Essentially corresponding to ceria doped with ca. 25% Nd_2O_3, and therefore an ionic conductor just like other rare earth doped cerias, it does not affect the overall resistive drop in our testing conditions; even if its conductivity could be one order of magnitude below that of 10-GDC, its thickness of only half a micron makes any additional ohmic drop to that of the 1 mm 10-GDC pellet negligible.

5. Conclusion

Sensitivity to contamination effects, in particular towards chromium and silicon, was revealed for Nd-nickelate based cathode material in the present study. The hypothesis that Cr-poisoning should be limited or even suppressed using alternative cathode materials free of Sr and Mn [2] has been invalidated here, and the electrochemical reduction of Cr-vapour species [3] appears independent of the cathode material. The findings indicating Cr-intolerance of Nd-nickelate will probably delay its use in SOFC, in contrast to electrolyzer cells [22], as long as the Cr-poisoning issue is not resolved by other means [23] than changing electrode materials.

Our results evidence additional degradation effects, in particular a synergistic decomposition of Nd-nickelate induced by raw powder contamination. Introduction of silicon has to be clearly avoided in early stages of SOFC processing to prevent Nd-nickelate decomposition into nickel oxide due to Nd-silicate formation. Finally, the material combination and high fabrication temperature of the nickelate–ceria interface does lead to an interfacial reaction layer before electrochemical testing; this layer, however, still a doped ceria ionic conductor, did not add here significant resistive effects due to its marginal thickness.

Acknowledgements

The Swiss Federal Office of Energy (contracts 153569,154156) is acknowledged for financial support. Many thanks to Fabienne Bobard for manipulating the FIB.

References

[1] E. Boehm, J.M. Bassat, P. Dordor, F. Mauvy, J.C. Grenier, Ph. Stevens, Solid State Ionics 176 (2005) 2717.
[2] T. Komatsu, H. Arai, R. Chiba, K. Nozawa, M. Arakawa, K. Sato, Electrochem. Solid-State Lett. 9 (2006) A9.
[3] K. Hilpert, D. Das, M. Miller, D.H. Peck, R. Weiss, J. Electrochem. Soc. 143 (1996) 3642.
[4] Y. Yang, E. Bucher, W. Sitte, J. Power Sources 196 (2011) 7313.
[5] J.A. Schuler, C. Gehrig, Z. Wuillemin, A.J. Schuler, J. Wochele, C. Ludwig, et al., J. Power Sources 196 (2011) 7225.
[6] A. Egger, E. Bucher, W. Sitte, C. Lalanne, J.M. Bassat, ECS. Trans. 25 (2009) 2547.
[7] E. Bucher, A. Egger, M. Yang, W. Sitte, Proc. 9th EFCF 7 (2010) 14.
[8] A. Egger, W. Sitte, F. Klauser, E. Bertel, J. Electrochem. Soc. 157 (2010) B1537.
[9] H. Luebbe, J. Van herle, H. Hofmann, P. Bowen, U. Aschauer, A. Schuler, et al., Solid State Ionics 180 (2009) 805.
[10] P. Tanasini, J.A. Schuler, Z. Wuillemin, M.L. Ben Ameur, C. Comninellis, J. Van herle, J. Power Sources 196 (2011) 7097.
[11] N. Nagata, Y. Itoh, H. Iwahara, Solid State Ionics 67 (1994) 215.
[12] J.A. Schuler, P. Tanasini, A. Hessler-Wyser, C. Comninellis, J. Van herle, Electrochem. Commun. 12 (2011) 1682.
[13] J.A. Schuler, Z. Wuillemin, A. Hessler-Wyser, J. Van herle, Electrochem. Solid-State Lett. 14 (2011) B20.
[14] J. Van herle, T. Horita, T. Kawada, N. Sakai, H. Yokokawa, M. Dokiya, Solid State Ionics 86–88 (1996) 1255.
[15] A. Holt, P. Kofstad, Solid State Ionics 69 (1994) 127.
[16] F. Mauvy, C. Lalanne, J.B. Bassat, J.C. Grenier, H. Zhao, L. Huo, et al., J. Electrochem. Soc. 153 (2006) A1547.
[17] J.A. Schuler, P. Tanasini, A. Hessler-Wyser, J. Van herle, Scr. Mater. 63 (2010) 895.
[18] H. Schwarz, Z. Allg. Chum. 322 (1963) 9.
[19] J.A. Schuler, Z. Wuillemin, A. Hessler-Wyser, J. Van herle, ECS. Trans. 25 (2009) 2845.
[20] Schuler JA. Master Thesis, EPFL; 2008.
[21] J. Hauck, K. Bickmann, K. Mika, Supercond. Sci. Technol. 11 (1998) 63.
[22] V.I. Sharma, B. Yildiz, J. Electrochem. Soc. 157 (2010) B441.
[23] Y. Matsuzaki, I. Yasuda, J. Electrochem. Soc. 148 (2001) A126.